

# Influence of composition and processing conditions on the morphology and properties of polyamide 6/ethylene–vinyl acetate copolymer blends

L. D'ORAZIO, C. MANCARELLA, E. MARTUSCELLI

*Istituto di Ricerche su Tecnologia dei Polimeri e Reologia del CNR, via Toiano 6, Arco Felice, Napoli, Italy*

A CASALE, A FILIPPI, F. SPERONI

*Tecnopolimeri, Ceriano Laghetto, Milano, Italy*

An ethylene–vinyl acetate copolymer has been mixed with polyamide 6 in a single screw extruder. The extrudate materials were processed according to two methods: extrusion by means of a capillary rheometer and injection moulding. The rheological properties of the blends and plain polymers, the mode and state of dispersion of the minor component and the impact properties of the polyamide 6-based blends were investigated. Different blend morphologies, strongly depending on the post-blending processing conditions and on the percentage wt/wt ethylene–vinyl acetate/polyamide 6, were observed by scanning electron microscopy. The impact behaviour of the injection moulded blends was correlated with the scanning electron microscopy analysis of the fracture surfaces.

## 1. Introduction

Melt blending of polyamide 6 (PA6) with different rubbery polymers is widely used for increasing the impact strength of polyamide 6 especially at low temperatures.

As found by Martuscelli and co-workers [1–3] and as reported in the literature by several other authors [4] a close interrelation exists between physico-mechanical properties and the phase structure of such blends. The macroscopically measured physico-mechanical characteristics are thought to depend on the average particle size, particle size distribution, structure of interphase regions and some molecular features (such as average molecular mass, degree of crosslinking, etc.) of the modifiers forming the dispersed phase in the mixture.

In the present paper we report the results of an investigation concerning the study of the melt rheology, morphology and impact properties of samples of blends of PA6 and ethylene–vinyl acetate copolymer (EVA) as functions of composition and post-blending processing (extrusion by means of a capillary rheometer and injection moulding). The work was undertaken with the aim of establishing correlations between the rheological characteristics of blends and plain polymers, composition, post-blending processing conditions, mode and state of dispersion of the minor component and some relevant mechanical properties such as the impact behaviour.

## 2. Experimental procedures

### 2.1. Materials

Nylon 6 (PA6) used throughout the work was Sniamid ASN 27/2 produced by Snia with a number average

molecular weight,  $\bar{M}_n$  of  $2.3 \times 10^4$ . The modifier was a commercial ethylene–vinyl acetate copolymer (EVA) made by Du Pont (trade name Elvax 250). The weight percentage of vinyl acetate and the melt flow index (ASTM D 1238) for Elvax 250 were 28.8 and 28.0 (g/10 min), respectively.

### 2.2. Blending

All blends investigated were obtained by mixing the components by means of a single-screw extruder (Gottfert;  $L/D = 25$  mm; diameter = 30 mm) at 50 r.p.m. at a temperature of 260°C.

The compositions examined are listed in Table I.

### 2.3. Sample preparation

The extrudate materials were processed according to two different methods: capillary extrusion and injection moulding. The capillary extrusion was performed at a very low shear rate by means of a capillary rheometer (Gottfert H K R 2000) equipped with a Dynisco pressure-transmitter. The samples were extruded without any capillary directly from the extrusion chamber through a die, having a diameter of 5.5 mm at 220, 240 and 260°C. Three different residence times ( $t_r$ ) (3, 6, 10 min) were used.

Injection moulded samples were obtained by means of an injection press (Negri and Bossi V79 F.A.). The

TABLE I Blend compositions investigated

Component	Blend code				
	A	B	C	D	E
PA6 (% wt/wt)	100	90	70	40	0
EVA (% wt/wt)	0	10	30	60	100

moulding temperatures were the same as those used for extrusion with the following  $t_r$  inside the cylinder of the press: 0, 3, 6 min. It was possible to extend  $t_r$  up to 10 min because of degradation of the EVA copolymer.

The rectangular shaped specimens obtained had the following dimensions: 13 mm wide, 62 mm long, 7 mm thick.

To perform Izod impact tests, a 0.50 mm deep notch with a tip radius of 0.25 mm was made on each sample.

## 2.4. Techniques

The overall morphology of the extrudate blends was investigated by means of a scanning electron microscope (SEM 501 Philips) on surfaces of cryogenically fractured samples. The fracture surfaces were coated with Au-Pd.

In order to achieve a better resolution of D blend morphology, an etching technique, based on the selective copolymer dissolution by means of xylene, was developed. The fracture surfaces of D blend were exposed to xylene vapour and subsequently prepared for SEM examination. It was observed that the copolymer was easily dissolved by xylene while the PA6 remained unaffected.

Izod impact tests were performed at room temperature on dry samples of injection moulded blends by using a fracture pendulum (Ceast Autographic Pendulum).

With a view to elucidate the influence of composition, injection moulding temperatures and  $t_r$  on both the overall morphology and the mode and mechanism of fracture, a morphological analysis of the Izod fractured surfaces was carried out.

## 3. Results and discussion

### 3.1. Rheological characterization

The constant force capillary rheometer was also employed for determining rheological characteristics of the pure homopolymers and of the blends. The samples were forced through a capillary of radius 0.5 mm and length 30 mm under an applied pressure of  $3 \times 10^6$  dyn cm<sup>-2</sup>. The shear rates at the walls,  $\dot{\gamma}_w$ , were measured at a given temperature. The viscosity values were calculated as the ratio of shear stress,  $\tau_w$ , to shear rate.

The rheological viscosities for PA6 were: 1100 P at 230°C; 850 P at 240°C and 600 P at 260°C; for the

TABLE II  $\dot{\gamma}_w$  and  $\eta$  values as a function of the extrusion temperature and  $t_r$  for B blends with  $\tau = 3 \times 10^6$  dyn cm<sup>-2</sup>

Temperature (°C)	$t_r$ (min)	$\dot{\gamma}_w$ (10 <sup>3</sup> sec <sup>-1</sup> )	$\eta$ (P)
220	3	9.5	317.7
	6	8.3	361.4
	10	9.0	333.3
240	3	9.0	333.3
	6	10.5	285.7
	10	9.05	331.5
260	3	10.5	285.7
	6	11.7	256.4
	10	13.0	230.7

TABLE III  $\dot{\gamma}_w$  and  $\eta$  values as a function of the extrusion temperature and  $t_r$  for C blends with  $\tau = 3 \times 10^6$  dyn cm<sup>-2</sup>

Temperature (°C)	$t_r$ (min)	$\dot{\gamma}_w$ (10 <sup>3</sup> sec <sup>-1</sup> )	$\eta$ (P)
220	3	30.9	97.1
	6	31.6	94.9
	10	31.3	95.8
240	3	30.3	99.0
	6	31.0	96.7
	10	30.9	97.1
260	3	31.0	96.7
	6	29.7	101.0
	10	30.5	98.4

EVA copolymer they were 260 P at 170°C and 175 P at 180°C.

It was impossible to carry out measurements at higher temperature because the copolymer became too fluid.

Blend samples were first melted at 240°C, then the shear rate values,  $\dot{\gamma}_w$ , were measured after  $t_r$  of 3, 6 and 10 min at three different temperatures: 220, 240 and 260°C. The applied shear stress,  $\tau_w$ , was constant at  $3 \times 10^6$  dyn cm<sup>-2</sup>.

The  $\dot{\gamma}_w$  and the  $\eta$  values for B, C and D blends are listed in Tables II to IV, respectively. As shown by Fig. 1, for a given shear stress and residence temperature the viscosity of blends is lower than that of PA6 and decreases with the increase of the EVA content. Furthermore, it may be observed that the values of viscosities seem not to be influenced systematically by  $t_r$ . Surprisingly it may be observed that viscosity of blends seems to be only slightly influenced by temperature at least in the range explored (220 to 260°C). This may be accounted for by:

1. modification of the mode and state of dispersion of the minor component;
2. degradation of EVA copolymer.

### 3.2. Phase morphology of the extruded samples

Scanning electron micrographs of cryogenical fractured surfaces of B blend extruded at 220°C with  $t_r$  of 3 and 10 min are shown in Figs. 2a and b, respectively.

For the shorter value of  $t_r$  (3 min) droplets of the EVA copolymer, uniformly distributed over the whole surfaces, with an average diameter of 1 to 2  $\mu$ m, are

TABLE IV  $\dot{\gamma}_w$  and  $\eta$  values as a function of the extrusion temperature and  $t_r$  for D blends with  $\tau = 3 \times 10^6$  dyn cm<sup>-2</sup>

Temperature (°C)	$t_r$ (min)	$\dot{\gamma}_w$ (10 <sup>3</sup> sec <sup>-1</sup> )	$\eta$ (P)
220	3	70.0	42.9
	6	61.0	49.2
	10	62.0	48.4
240	3	54.0	55.6
	6	71.0	42.2
	10	65.0	46.1
260	3	65.0	46.1
	6	60.0	50.0
	10	80.0	37.5

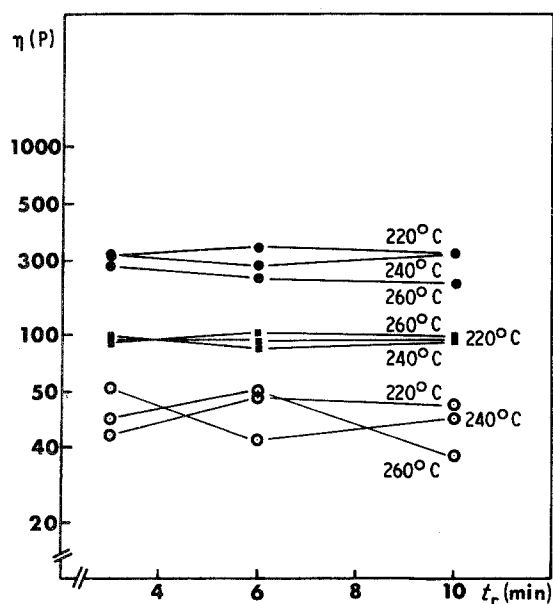


Figure 1 Viscosity values for all the blends investigated as a function of residence time. ●, PA6/EVA, 90/10; ■, PA6/EVA, 70/30; ○, PA6/EVA, 40/60.

observed. The presence of cavities with smooth walls indicated poor adhesion between particles and matrix.

For the longer  $t_r$  value (10 min) the dispersed phase tends to be elongated along the extrusion direction assuming an ellipsoidal shape (Fig. 2b). Dispersed particles with larger size (average diameter 1 to 4  $\mu\text{m}$ ) are observed in B blend at 260°C. For such extrusion temperatures an increase of  $t_r$  does not seem to cause any shape deformation of the particles (compare Figs. 3a and b). This last behaviour may probably be related to the lower viscosities of the blends extruded at 260°C (see Table II).

Scanning electron micrographs of the fractured surfaces of C blend extruded at 220°C, with different  $t_r$ , are reported in Fig. 4. In the case of blends with  $t_r = 3$  min it is found that the mode of dispersion and the size distribution of the dispersed particles are similar to that of B blend extruded under the same conditions (compare Figs. 2a and 4a).

A drastic change in the overall morphology is observed when the C blends are extruded at 220°C but

with a  $t_r$  value of 10 min. The copolymer, as matter of fact, segregates in cylindrical-shaped domains oriented along the flow direction (see Fig. 4b).

On raising the extrusion temperature to 260°C, irrespective of the  $t_r$  value, C blends exhibit a droplet-like morphology (compare Figs. 5a and b). It is remarkable that, with respect to the same blend processed at 220°C, the EVA inclusions show a larger average diameter (2 to 5  $\mu\text{m}$ ) (compare Figs. 4 and 5). On the walls of the cavities and on the surfaces of the EVA domains, PA6 spherulites and spherulites prints can be observed (see Fig. 5b). The above observations suggest that the nucleation process of the PA6 spherulites may begin at the interface between dispersed phase and matrix.

Micrographs of fractured surfaces of the extrudate of D blends processed at 220°C with  $t_r = 3$  min and 10 min are shown in Figs. 6 and 7.

The selective dissolution of the EVA copolymer with boiling xylene vapour shows that at this composition the copolymer represents the continuous phase including the polyamide as dispersed phase (Figs. 6a and b).

As shown by Figs. 7a and b, the PA6 dispersed phase is elongated along the extrusion direction giving rise to irregular rods in regions closer to the border of the filament, while it assumes a spherical shape going towards the centre of the sample. Inside the rods, small particles of EVA (average diameter < 1  $\mu\text{m}$ ) seem to be occluded. Furthermore, as indicated by the very smooth surfaces of PA6 domains, there is scanty adhesion between the matrix and the dispersed phase (see Fig. 7b).

It is interesting to point out that by increasing  $t_r$ , the probability to observe rods, even in regions closer to the centre of the filament, highly increases (see Fig. 7c).

At higher extrusion temperature, rods of PA6 oriented along the flow direction are observed in the region next to the edge of the filament, while in the middle of the sample the PA6 forms spherical domains (see Figs. 8a and b). On the surfaces of PA6 domains spherulites are clearly visible (see Fig. 8c). It is to be noted that at 260°C the dispersion mode of polyamide is unaffected by  $t_r$ .

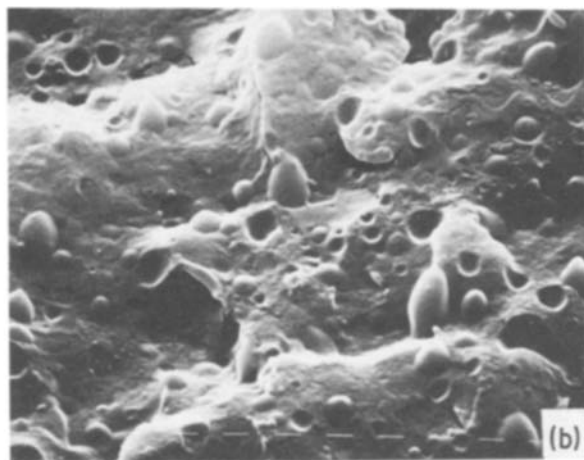


Figure 2 Scanning electron micrographs of cryogenic fracture surfaces of B blend extruded at 220°C with different residence times: (a) 3 min,  $\times 3750$ ; (b) 10 min,  $\times 3750$ .

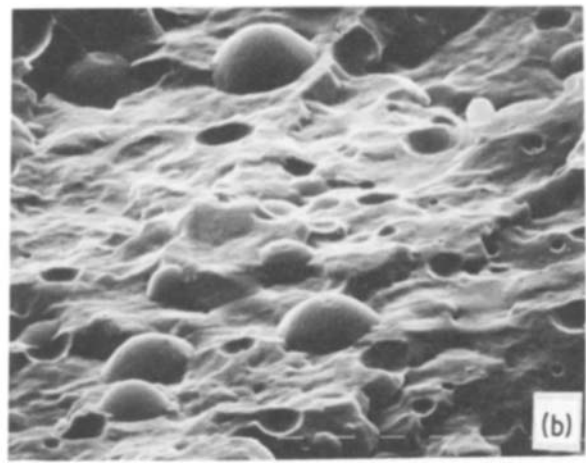
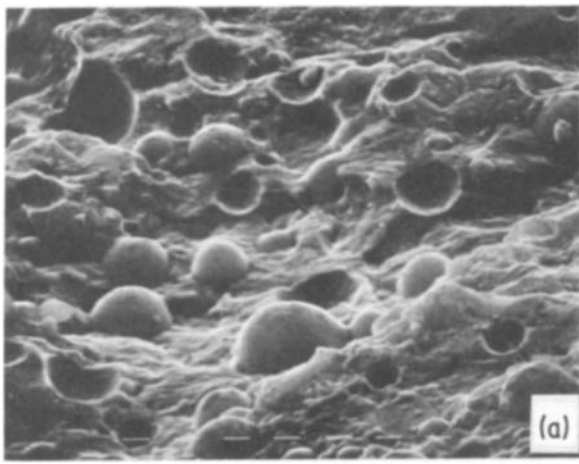


Figure 3 Scanning electron micrographs of cryogenic fracture surfaces of B blend extruded at 260°C with different residence times: (a) 3 min,  $\times 3750$ ; (b) 10 min,  $\times 3750$ .

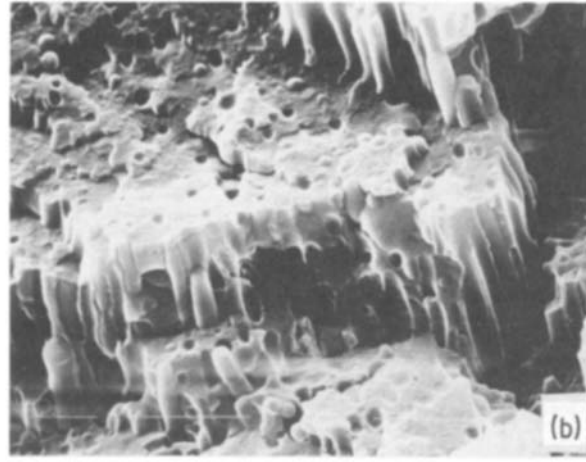
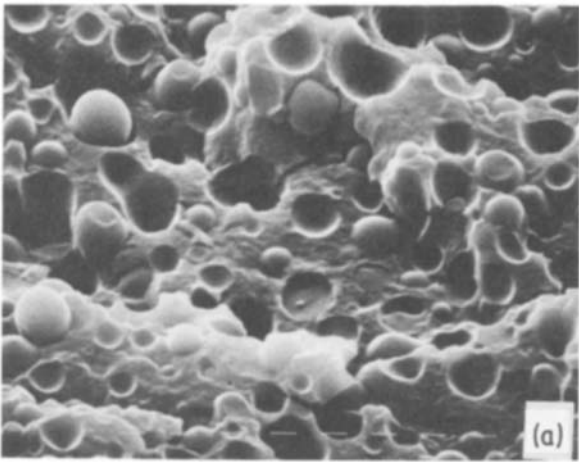


Figure 4 Scanning electron micrographs of cryogenic fracture surfaces of C blend extruded at 220°C with different residence times: (a) 3 min,  $\times 3750$ ; (b) 10 min,  $\times 1875$ .

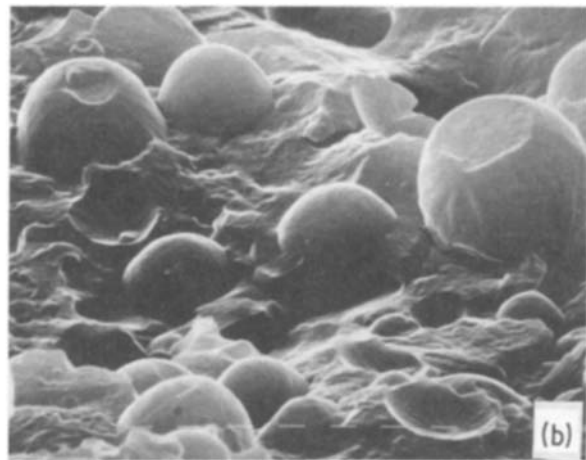
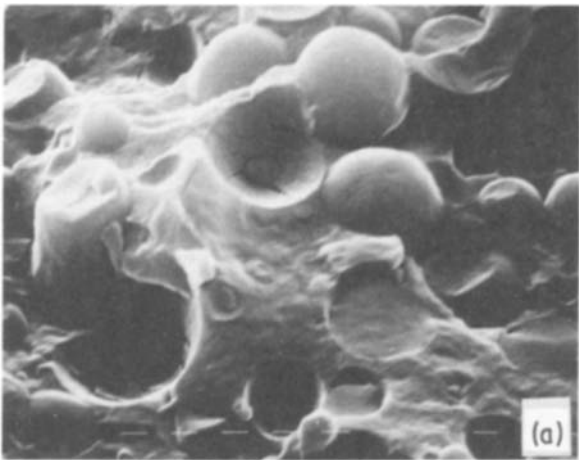


Figure 5 Scanning electron micrographs of cryogenic fracture surfaces of C blend extruded at 260°C with different residence times: (a) 3 min,  $\times 3750$ ; (b) 10 min,  $\times 3750$ .

The finding that in blends with EVA matrix the dispersed PA6 may more easily form rod-like structures is probably related to the low value of the phase viscosity ratio  $\eta_{EVA}/\eta_{PA6}$  ( $\eta_{EVA} \ll \eta_{PA6}$ ).

The larger probability of finding rods of the PA6 dispersed phase in the vicinity of the viscometer wall is accounted for by the fact that in such regions  $\dot{\gamma}$  is larger.

### 3.3. Morphology of fractured surfaces of injection-moulded samples

The fracture surfaces of PA6 homopolymer broken at room temperature show a distinct induction region starting from the middle of the notch and covering a limited area where the PA6 undergoes a plastic deformation (see Fig. 9a). The remainder of the sample exhibits a rough topography typical of a fast fracture.

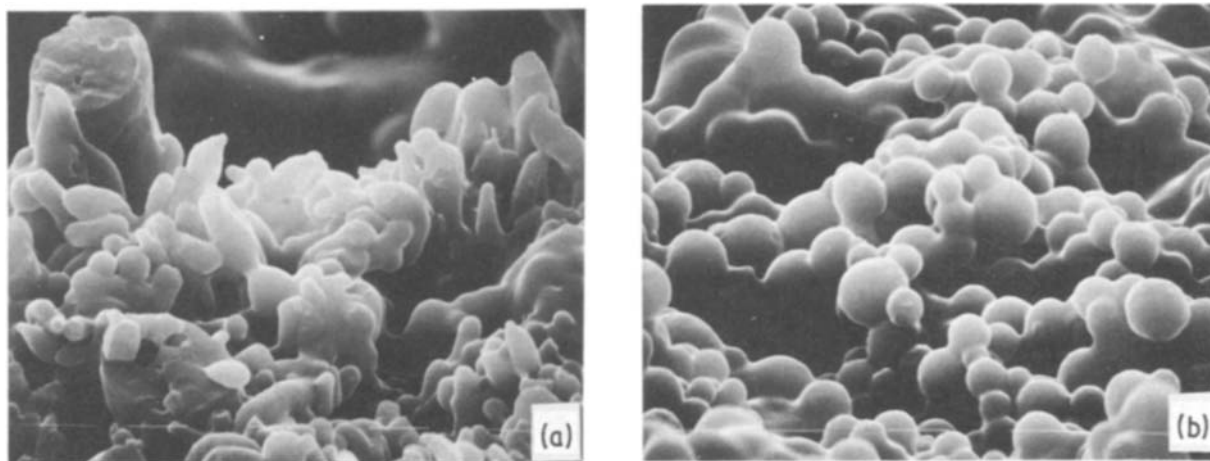


Figure 6 Scanning electron micrographs of cryogenic fracture surfaces of D blend after etching with xylene vapours: (a) border,  $\times 938$ ; (b) central part,  $\times 938$ .

No evidence of stress whitening is observed. These findings indicate that at room temperature the impact energy is mainly related to the yielding process in the induction region. As shown in Figs. 9b and c the polyamide crystallizes in spherulitic superstructure; the size of such spherulites seems to be larger for higher processing temperatures. The residence time does not seem to affect the PA6 superstructure and its fracture behaviour.

Examination of the fractured surfaces of B blends reveals an induction region around the notch showing a stress whitening phenomenon. Such observation

indicates the formation of multicrazes during the test. It can be observed, in addition, that the matrix is also plastically deformed (see Fig. 10a). The regions far from the notch show a morphology typical of a brittle fracture (see Fig. 10b).

This morphological evidence suggests that the fracture mode of B blends, in the induction region, is the result of the combined effect of multicraze propagation and shear yielding. Such a process is followed by a rapid crack propagation involving the rest of the sample.

The size of the EVA inclusions (average diameter ranging from 1 to 2  $\mu\text{m}$ ) indicates the fine and homogeneous mode of the copolymer dispersion in the matrix.

It is to be noted that the moulding temperature and/or residence time do not influence the fracture surface morphology of such a blend (compare Figs. 10b and d with Figs. 11a and b).

Fracture surfaces of C blends show a limited induction region starting from the middle of the notch; with respect to B blend, a slighter stress whitening phenomenon in the induction area is observed. This

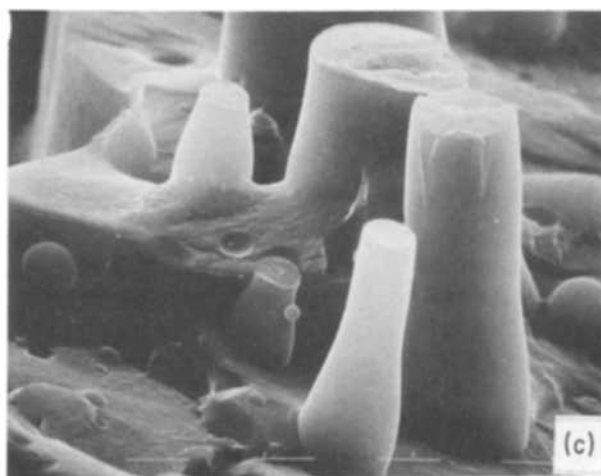
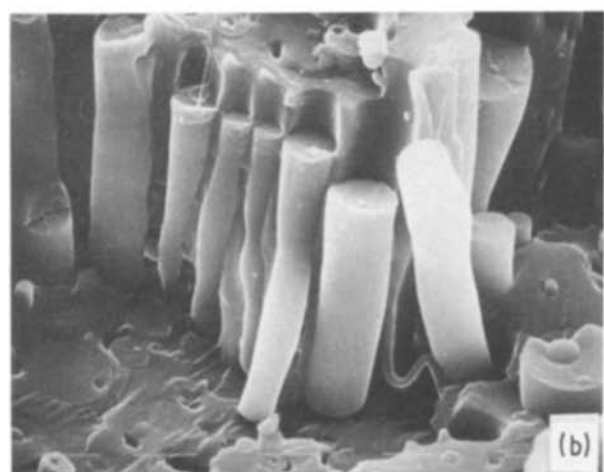
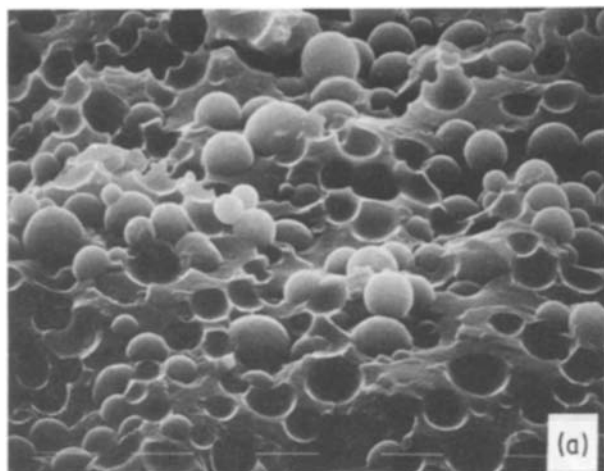
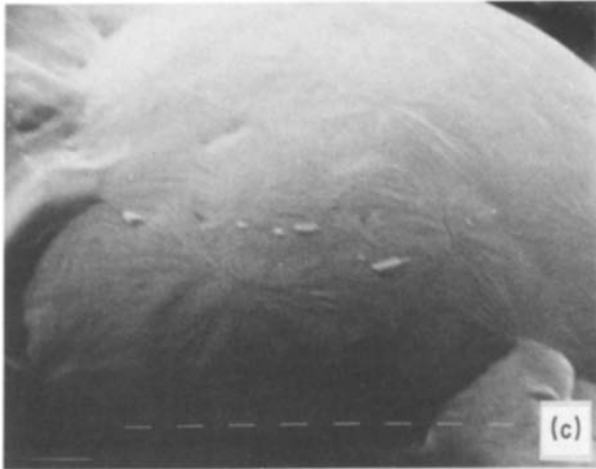
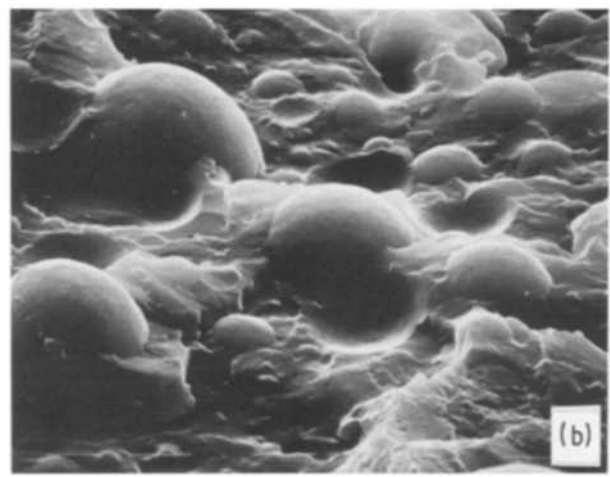
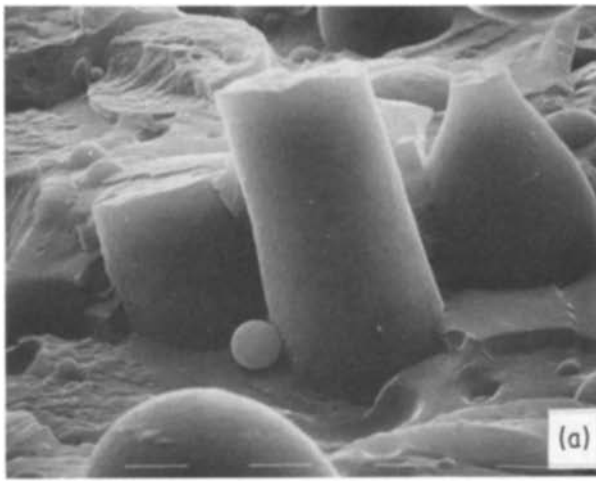
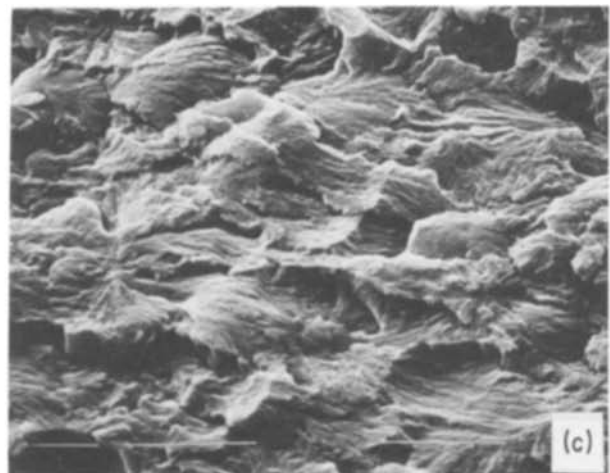
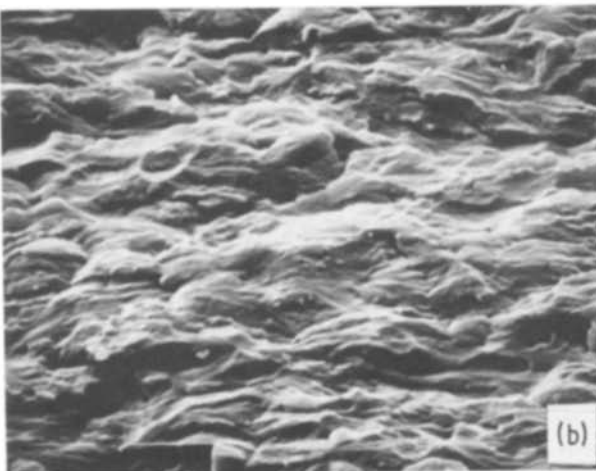
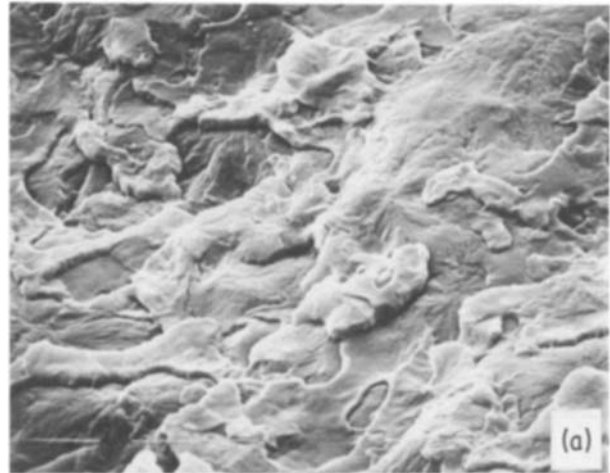


Figure 7 Scanning electron micrographs of cryogenic fracture surfaces of D blend extruded at 220°C with different residence times: (a) 3 min, central part,  $\times 1063$ ; (b) 3 min, border,  $\times 1063$ ; (c) 10 min, border,  $\times 1063$ .



*Figure 8* Scanning electron micrographs of cryogenic fracture surfaces of D blend extruded at 260°C with different residence times: (a) 3 min,  $\times 1063$ ; (b) 10 min,  $\times 1063$ ; (c) 10 min,  $\times 4250$ .

*Figure 9* Scanning electron micrographs of Izod fracture surfaces of the homopolymer at different injection-moulding temperatures with 6 min of residence time: (a) 260°C, induction region,  $\times 2125$ ; (b) 220°C, propagation region,  $\times 2125$ ; (c) 260°C, propagation region,  $\times 2125$ .



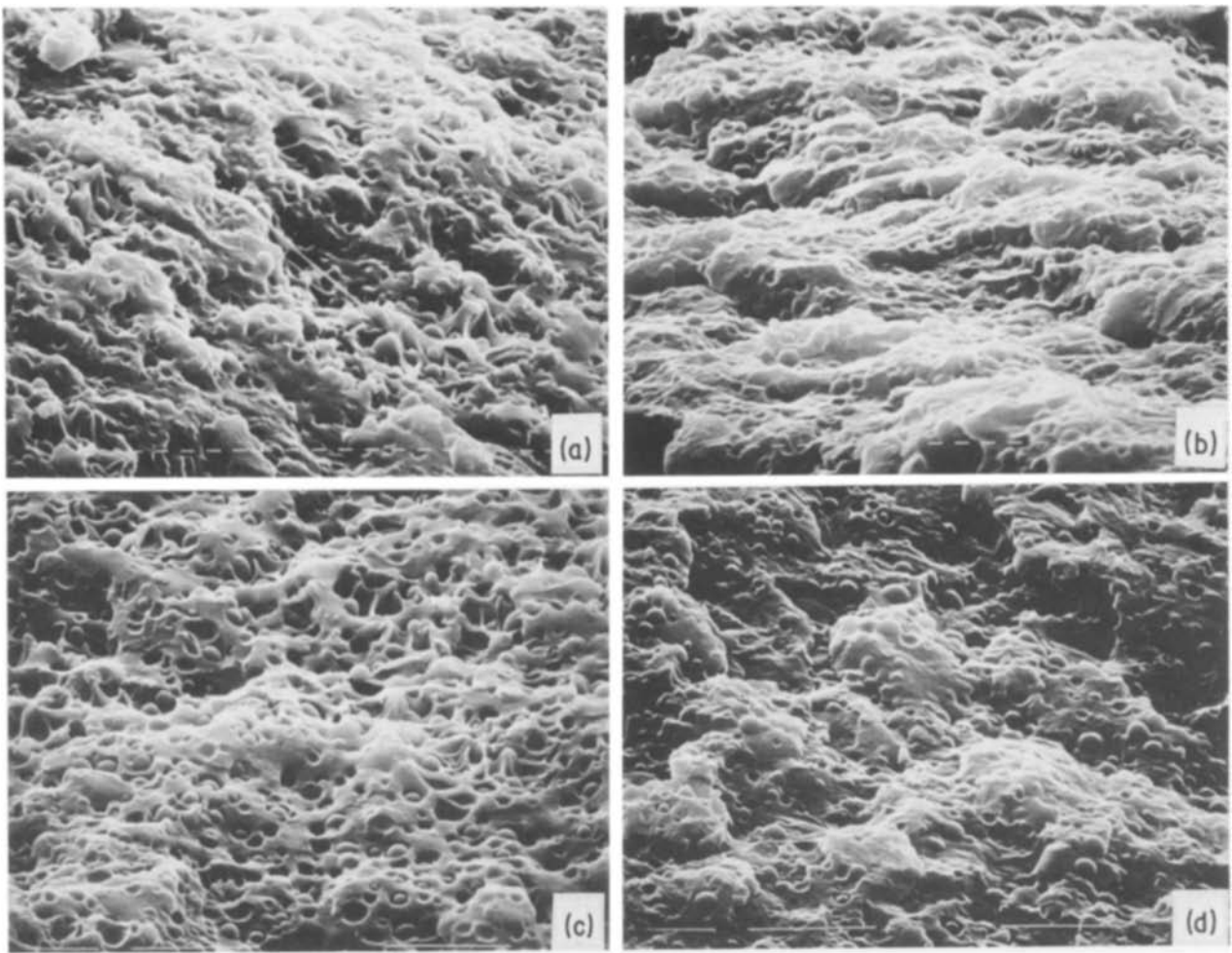


Figure 10 Scanning electron micrographs of Izod fracture surfaces of B blend moulded at 260° C with 0 and 6 min residence times: (a) 0 min, induction region, × 1875; (b) 0 min, propagation region, × 1875; (c) 6 min, induction region, × 1875; (d) 6 min, propagation region, × 1875.

finding indicates that the multicraze fracture mechanism is less active in avoiding catastrophic fracture.

As shown in Fig. 12, by adding 30% EVA copolymer, a homogenous dispersion is achieved again, but the size of the inclusion is larger (particle diameter ranging from 1 to 5  $\mu\text{m}$ ).

As occurs for B blends, the mode of dispersion of the copolymer is unaffected by increasing processing temperature and/or extending the residence time.

### 3.4. Izod impact test

The values of the Izod impact strength ( $R$ ) for plain polyamide and for all the blends investigated are reported as a function of composition in Figs. 13 to 15. For a given value of  $t_r$ , the PA6 homopolymer exhibits  $R$  values slightly decreasing with increasing processing temperature. Furthermore, the extension of the residence time affects only the impact behaviour of the PA6 processed at lower temperatures. In fact,

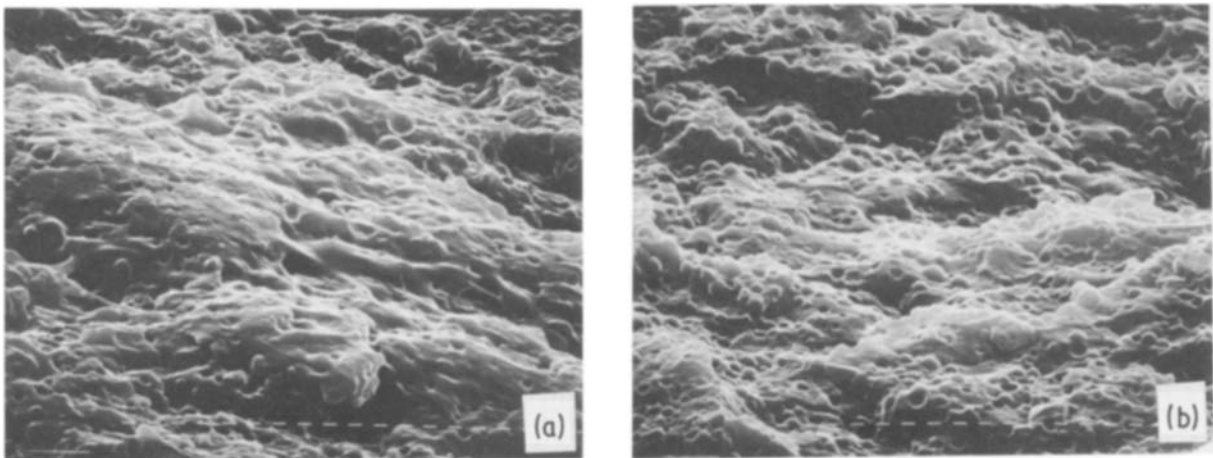


Figure 11 Scanning electron micrographs of Izod fracture surfaces of B blend moulded at 220° C with 0 and 6 min of residence times: (a) 0 min, propagation region, × 1875; (b) 6 min, propagation region, × 1875.

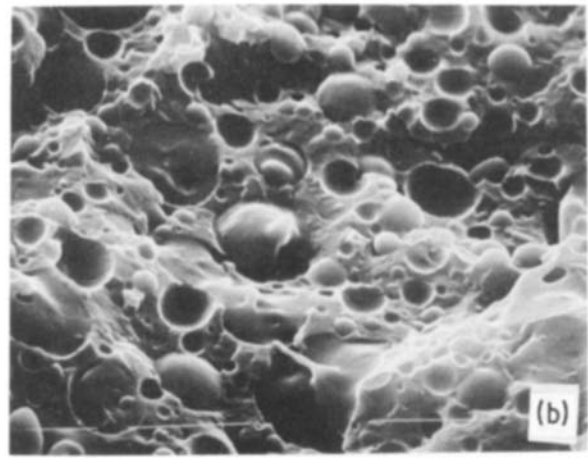
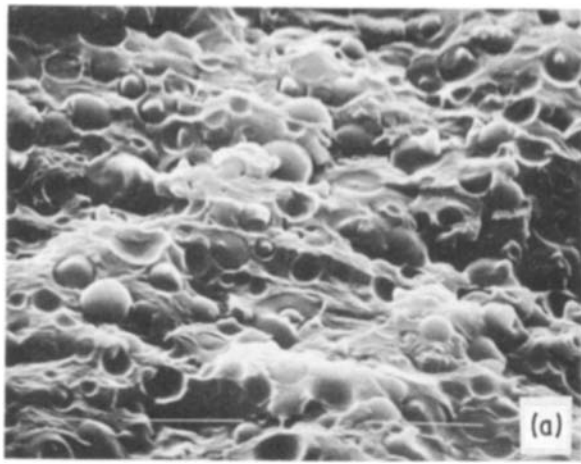


Figure 12 Scanning electron micrographs of Izod fracture surfaces of C blend moulded at 260 and 220°C, respectively, with a residence time of 6 min: (a) 260°C, propagation region  $\times 1875$ ; (b) 220°C, propagation region  $\times 1875$ .

a slight increase in  $R$  with longer residence time is observed. Such behaviour is likely to be related to the crystallization conditions and to the spherulite size as suggested by the morphological investigation.

By adding 10% wt/wt EVA copolymer to the PA6, an improvement in  $R$  equivalent to  $3 \text{ kg cm cm}^{-2}$  is achieved (see Figs. 13 to 15). Such a result is in agreement with the fractographic analysis showing that in the presence of the EVA particles, diffuse shear yielding is accompanied by multicraze formation during the fracture. The main role of the EVA domains is to induce high local stress concentration, so dissipating the fracture energy and diverting the ultimate catastrophic crack.

Enhancing the copolymer content in the blends, contrary to expectation, the impact resistance values are lower than those observed in the case of blends containing 10% EVA.

Such a behaviour may be accounted for by considering that the effectiveness of the impact improvements strongly depends, among the other variables, on the average size of the dispersed particles. Generally, for a given polymer pair, there will be an optimum size

of the dispersed domains that yields optimum toughness [5]. Thus the maximum observed in the value of  $R$  for 90/10 PA6/EVA blend is likely to be ascribed to the fact emerging from the morphological investigation, that the dimensions of EVA domains are, in the case of blends with higher copolymer content, larger than the optimum size.

This also explains why the fracture mechanism based on the formation and propagation of multicraze is exhibited by such blends to a lesser extent, as shown by comparison of the material volume involved to the stress whitening phenomenon.

Another possible explanation of the observed fall in the values of  $R$  may be the poor adhesion between PA6 and EVA. A poorly bonded dispersed phase would weaken the structure as the EVA particles act like a fine dispersion of voids.

Furthermore, the observation that  $R$  decreases upon increasing the residence time, especially for 70/30 blends, is probably related to the degradation processes of blend components and/or to changes in the structure and morphology of the PA6 matrix [6, 7].

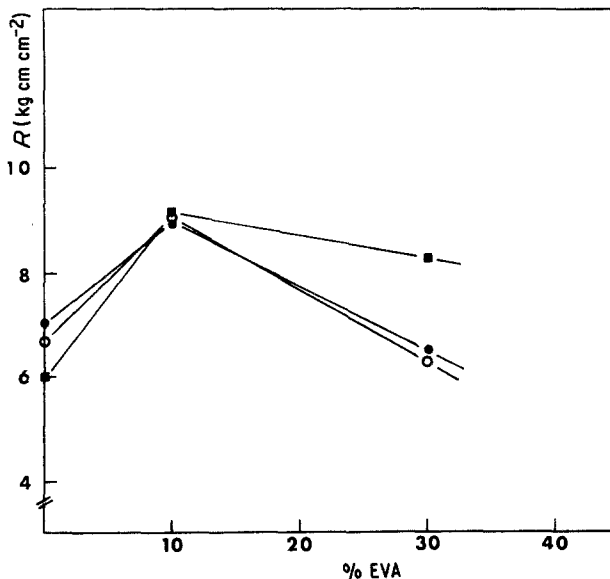


Figure 13 Izod impact strength values ( $R$ ) for the PA6, B and C blends, moulded at 220°C with different residence times, as a function of composition. ■,  $t_r = 0$  sec; ●,  $t_r = 180$  sec; ○,  $t_r = 360$  sec.

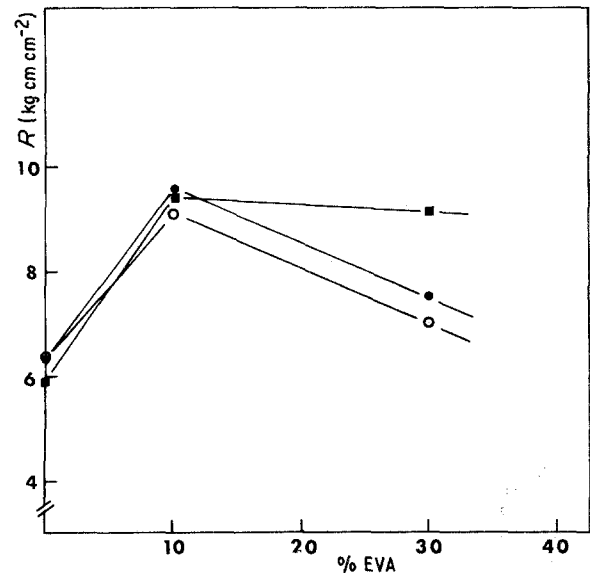


Figure 14 Izod impact strength values ( $R$ ) for the PA6, B and C blends, moulded at 240°C with different residence times, as a function of composition. ■,  $t_r = 0$  sec; ○,  $t_r = 180$  sec; ●,  $t_r = 360$  sec.



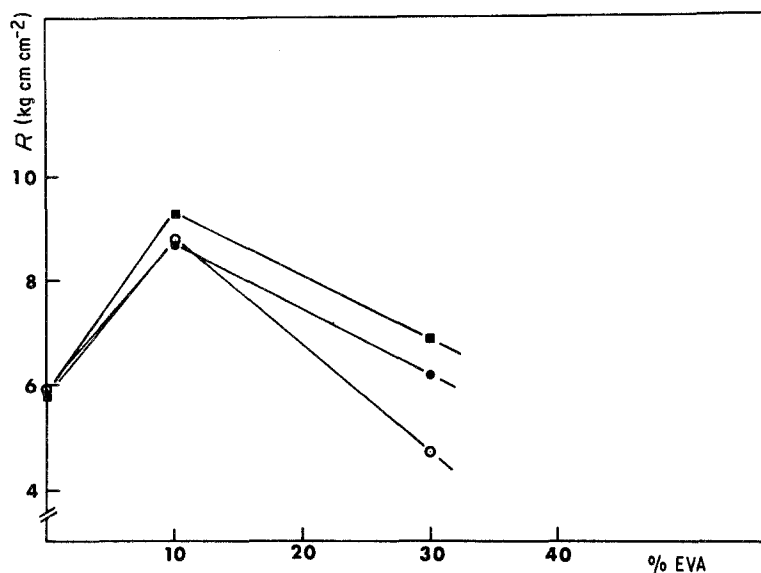


Figure 15 Izod impact strength values ( $R$ ) for the PA6, B and C blends, moulded at 260°C with different residence times, as a function of composition. ■,  $t_r = 0$  sec; ●,  $t_r = 180$  sec; ○  $t_r = 360$  sec.

### Acknowledgement

This work was partly supported by "Progetto Finalizzato Chimica Fine e Secondaria, CNR.

### References

1. S. CIMMINO, L. D'ORAZIO, R. GRECO, G. MAGLIO, M. MALINCONICO, C. MANCARELLA, E. MARTUSCELLI, R. PALUMBO and G. RAGOSTA, *Polym. Eng. Sci.* **24** (1984) 1.
2. C. CIMMINO, L. D'ORAZIO, R. GRECO, G. MAGLIO, M. MALINCONICO, C. MANCARELLA, E. MARTUSCELLI, P. MUSTO, R. PALUMBO and G. RAGOSTA, *ibid.* **25** (1985) 4.
3. G. ILLING, in "Polymer Blends: Processing, Morphology and Properties", edited by E. Martuscelli, R. Palumbo and M. Kryszewski, (Plenum Press, New York, 1980) p. 167.
4. F. IDE and A. HASEGAWA, *J. Appl. Polym. Sci.* **18** (1974) 963.
5. C. B. BUCKNALL, in "Toughened Plastics" (Applied Science, London, 1977).
6. E. MARTUSCELLI, *Polym. Eng. Sci.* **24** (1984) 8.
7. E. MARTUSCELLI, F. RIVA, C. SELLITTI and C. SILVESTRE, *Polymer* **26** (1985) 270.

Received 24 January  
and accepted 30 May 1985